ELSEVIER

Journal of Photochemistry and Photobiology A: Chemistry 124 (1999) 95–99

Journal of Photochemistry and Photobiology A:Chemistry

Photodynamic action of some naturally occurring quinones: formation of reactive oxygen species

J. Johnson Inbaraj, R. Gandhidasan, R. Murugesan*

School of Chemistry, Madurai Kamaraj University, Madurai 625021, India

Received 4 November 1998; received in revised form 18 January 1999; accepted 5 February 1999

Abstract

Four naturally occurring quinones, thespone (TP), thespesone (TPE), mansonone-D (MD) and mansonone-H (MH), extracted from the heartwood of *Thespesia populnea*, are studied for their ability to generate superoxide anion radical ($O_2^{-\bullet}$) and singlet oxygen ($^1O_2$) upon photoirradiation. The generation of $^1O_2$ is followed by *N*,*N*-dimethyl-4-nitrosoaniline (RNO) bleaching assay. Relative to rose bengal, singlet oxygen generating efficiencies of TP, MD, MH and TPE are found to be 0.30, 0.13, 0.03 and 0.01, respectively. The formation of $O_2^{-\bullet}$ is monitored by optical spectroscopy using SOD inhibitable cytochrome *c* reduction assay. Generation of $O_2^{-\bullet}$ radical is effectively enhanced by the presence of electron donors such as EDTA and DETAPAC. Photolysis of TP, MD, TPE and MH in DMSO, in the presence of 5,5-dimethyl-1-pyrroline-*N*-oxide (DMPO) generates 12-line EPR spectra characteristic of $O_2^{-\bullet}$. EPR spectral studies show the formation of both light dependent and 'dark' radicals. Our results indicate that both TP and MD possess high ability to generate reactive oxygen species.

Keywords: Spin trapping; 5,5-Dimethyl-1-pyrroline-*N*-oxide (DMPO); Free radicals; Superoxide anion radical; Singlet oxygen

1. Introduction

Photosensitisation by many anticancer agents such as hematoporphyrin derivatives [1,2] and anthrapyrazoles [3–5] has been demonstrated. In recent years, considerable attention is paid to the promising use of quinones in photosensitisation of human malignancies [6,7]. Photoinduced production of superoxide anion radicals by adriamycin and daunorubicin is well known [8]. Phleichrome, a quinonoid agent has been shown to photogenerate $^1O_2$ by energy transfer from its photoexcited triplet state to molecular oxygen (Type II process). Phleichrome also generates $O_2^{-\bullet}$ via an electron transfer process (Type I) from its excited state, upon exposure to light [9]. Recently, we have investigated some naturally occurring quinones for their cytotoxic action against human breast adenocarcinoma cell line (MCF7) [10]. These quinones generate $O_2^{-\bullet}$ upon enzymatic reduction. Due to the current interest in photosensitisation by quinones [6], the present study reports the photogeneration of $^1O_2$ and $O_2^{-\bullet}$ from these quinones. Effect of electron donors such as ethylenediaminetetraacetic acid (EDTA) and diethylenetriaminepentaacetic acid (DETAPAC) on the efficiencies of generation of $O_2^{-\bullet}$, is also presented here.

2. Experimental

2.1. Chemicals

Quinones, used in this study were extracted, following the reported procedure [11], from the reddish brown heartwood and roots of *Thespesia populnea*, collected from the Mayavaram area (Tanjore District) of Tamil Nadu, India. Structures of these quinones are given in Fig. 1.

N,*N*-Dimethyl-4-nitrosoaniline (RNO), 5,5-dimethyl-1-pyrroline-*N*-oxide (DMPO), 1,4-diazabicyclo[2,2,2]octane (DABCO) and rose bengal (RB) were obtained from Aldrich. Superoxide dismutase (SOD) and catalase were purchased from Sigma. Dimethyl sulphoxide (HPLC grade) from Qualigens Fine Chemicals, India was used. Imidazole obtained from S.D. Fine Chemicals, India, was used after repeated recrystallisation from water. Doubly distilled water was used for all the experiments. DMPO was purified using activated charcoal [12]. The concentration of the spin trap DMPO was determined spectrophotometrically using $\varepsilon_{227} = 8000\ M^{-1}\ cm^{-1}$.

*Corresponding author. Tel.: +91-452-858246; fax: +91-452-859105; e-mail: mkubic6@giasmd01.vsnl.net.in

1010-6030/99/$ – see front matter
PII: S1010-6030(99)00040-4

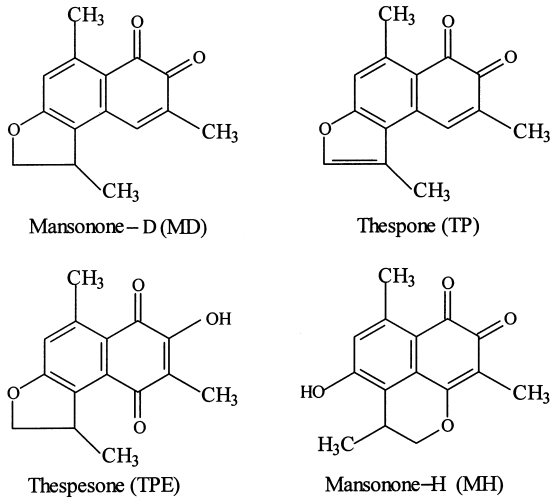

Fig. 1. Structures of thespone, thespesone, mansonone-D and mansonone-H.

2.2. Detection of singlet oxygen

The detection of singlet oxygen was performed by the method developed by Kraljic and El Mohsni [13]. The sensitisers were exposed to light in the presence of imidazole (10 mM) and RNO (50 mM) in a 50 mM phosphate buffer (pH = 7.4). The formation of $^1O_2$ was monitored spectrophotometrically by following the bleaching of RNO at 440 nm by the transannular peroxide intermediate, formed as a result of reaction between photogenerated $^1O_2$ and imidazole. Shimadzu UV-VIS spectrometer (UV-160) was used for optical measurements.

The rate of disappearance of quencher (A) obeys the following equation [14]

$$-\frac{d[A]}{dt} = (I_{ab}\Phi\,{}^1O_2)\frac{k_r[A]}{k_d}$$

where, k_r is the rate constant for chemical quenching, k_d is the rate constant for deactivation of $^1O_2$ by the solvent and I_{ab} is the intensity of light absorbed by the sensitiser. The slope of the first order plot is $I_{ab}\Phi\,{}^1O_2(k_r/k_d)$. The slope was calculated by fitting the experimental data to a second order polynomial using a MATLAB program. Decay of A was studied for each quinone and also for the well known singlet oxygen generator RB under identical conditions. The relative ratio of the slopes of the quinones to RB, after correction for molar absorption and photon energy [15], gives the relative efficiency of singlet oxygen generation. In this calculation, the $^1O_2$ quantum yield of RB [16] was taken to be 0.76. Interference of $O_2^{-\bullet}$ and H_2O_2 in the RNO bleaching was eliminated by adding SOD and catalase.

2.3. Light source

Light source used for irradiation was a 150 W xenon lamp. A filter combination of 10 cm potassium iodide solution (0.1 g in 100 ml) and 1 cm pyridine was used to cut off below 300 nm and to achieve a spectral window of 300–700 nm. The irradiation was generally carried out in an open cuvette in equilibrium with the atmosphere.

2.4. Detection of superoxide anion

2.4.1. EPR spin trapping

EPR spectra were recorded using a Varian E-109 century line EPR spectrometer operating at X-band frequency with 100 kHz modulation at room temperature. Solution of quinone (100 μM) and DMPO (100 mM) in DMSO, placed in a quartz cuvette, was continuously stirred using a magnetic stirrer during irradiation. Irradiated solution was drawn into a flat aqueous cell for EPR measurements. The microwave power was maintained at 20 mW and the modulation amplitude was kept at 0.05 mT. EPR spectra from spin trapping experiments often require simulation to find the hyperfine coupling constants. A BASIC computer program was used to simulate the EPR spectra. The output from this program was plotted using a MATLAB program to get the simulated spectra.

2.4.2. SOD inhibitable cytochrome c reduction

Formation of superoxide was assayed also using the SOD inhibitable cytochrome *c* reduction method. Quinones were photolysed in the presence of ferricytochrome *c* (40 μM) in 50 mM phosphate buffer (pH = 7.4). The reduction was monitored spectrophotometrically at 550 nm using $\Delta OD_{550} = 20\,000\ M^{-1}\,cm^{-1}$ for reduced–oxidised cytochrome *c* [17].

3. Results and discussion

The absorption spectra of the quinones in DMSO, showed strong bands around 280 and 400 nm. The band around 400 nm is characteristic of the *o*-quinone moiety [11].

3.1. Singlet oxygen generation

The rate of bleaching of RNO as a function of irradiation time is shown in Fig. 2 for the quinones. Bleaching by RB is also included in this figure which gives the raw data for the RNO bleaching at 440 nm. The ratio of the slopes of RB to each quinone was corrected for molar absorption and photon energy to obtain the relative singlet oxygen generating efficiencies of the quinones. The relative yields thus evaluated are, 0.30, 0.13, 0.03 and 0.01 for TP, MD, MH and TPE, respectively.

To confirm the formation of $^1O_2$, bleaching of RNO was carried out in the presence of DABCO, a specific singlet oxygen quencher. Fig. 3 shows the rate of bleaching of RNO by TP in the presence of equimolar amounts of imidazole and DABCO (10 mM). Both DABCO and imidazole are known to have almost comparable rate [18] of quenching of $^1O_2$. From Fig. 3, the ratio of the slopes of RNO bleaching in the presence and absence of DABCO is found to be nearly

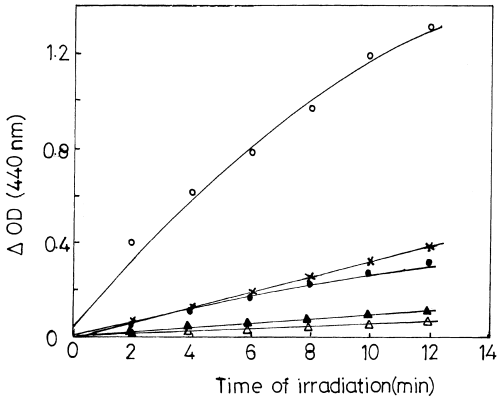

Fig. 2. Photosensitised RNO bleaching measured at 440 nm as a function of irradiation time in minutes in the presence of imidazole (10 mM) in 50 mM phosphate buffer, pH 7.4 by RB (○ ○ ○), MD (x x x), TP (● ● ●),TPE (Δ Δ Δ) and MH (▲ ▲ ▲).

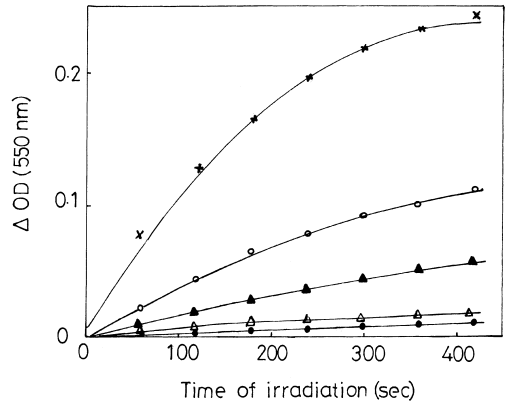

Fig. 4. Photosensitised superoxide generation measured as the rate of cytochrome *c* reduction in the presence of ferricytochrome *c* (40 μM) in 50 mM phosphate buffer, pH 7.4, with MD (x x x), TP (○ ○ ○), MH (▲ ▲ ▲) TPE (Δ Δ Δ) and MD + SOD (● ● ●) as a function of irradiation time.

half, thus confirming the generation of $^1O_2$ during the photosensitisation process.

It is known that RNO is also bleached by hydroxyl radical [19]. The hydroxyl radical can be generated from $O_2^{-\bullet}$ via iron catalysed Fenton reaction as shown in the following reaction scheme [20]

$$O_2^{-\bullet} + 2H^+ \rightarrow H_2O_2$$

$$Fe^{3+} + O_2^{-\bullet} \rightarrow Fe^{2+} + O_2$$

$$Fe^{2+} + H_2O_2 \rightarrow Fe^{3+} + OH^{\bullet} + OH^-$$

The contribution of OH radicals in bleaching of RNO could be minimised by using metal chelates such as DETAPAC and EDTA, which render the metal ion redox inactive. However, since both could participate in electron transfer reactions with the excited sensitiser molecule (as discussed later) this could lead to additional difficulties. Addition of SOD and catalase, which remove $O_2^{-\bullet}$ and H_2O_2 from the reaction mixture, respectively, could permit the detection and quantification of $^1O^2$ production, without interference from OH radical. Nevertheless, the same experiment was carried out in the presence of specific hydroxyl radical scavenger such as ethanol [21]. Addition of ethanol had no effect on the RNO bleaching (data not shown) indicating that hydroxyl radical is not generated during photosensitised reaction of these quinones, under our experimental conditions.

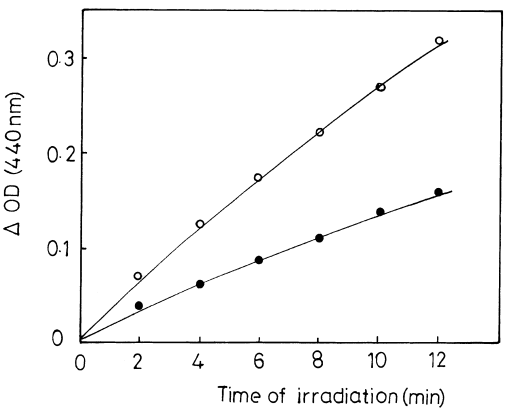

Fig. 3. Photosensitised RNO bleaching by TP in the absence (○ ○ ○) and presence (● ● ●) of 0.01 M DABCO.

3.2. Superoxide generation

Generation of $O_2^{-\bullet}$ from these quinones on photoillumination, could be readily studied by following the ferricytochrome *c* reduction efficiencies. Fig. 4 shows the raw data for the rate of cytochrome *c* reduction when air saturated solutions of the quinones were photolysed in the presence of 40 μM cytochrome *c* in phosphate buffer (50 mM). TP, MD, MH and TPE were found to reduce cytochrome *c* with different efficiencies. After correction for molar absorption, the rates of superoxide anion generation by TP, MD, MH and TPE were derived to be 0.0375, 0.0357, 0.0074 and 0.0025 μM/s, respectively. Addition of SOD (50 μg/ml) was found to inhibit the cytochrome *c* reduction (Fig. 4). Control experiments indicated that quinone, oxygen and light were all essential for the reduction of ferricytochrome *c*.

Further the effect of electron donors such as EDTA and DETAPAC on the efficiencies of $O_2^{-\bullet}$ production was also studied, using cytochrome *c* reduction assay. Fig. 5 shows the effect of EDTA on the cytochrome *c* reduction by TP, TPE, MD and MH. The electron donor, EDTA, enhanced the rate of cytochrome *c* reduction. The rates were found to be 0.1930, 0.1696, 0.0142 and 0.0075 μM/s for TP, MD, MH and TPE, respectively. In a similar experiment, the related electron donor, DETAPAC, was also found to participate in electron transfer process and enhance the $O_2^{-\bullet}$ generation by the sensitiser MD, but to a lesser extent than EDTA. Enhancement of generation of $O_2^{-\bullet}$ in the presence of

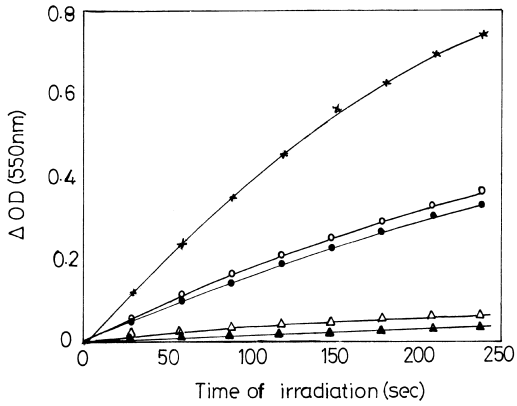

Fig. 5. Photosensitised cytochrome *c* reduction in the presence of EDTA by MD (x x x), TP (○ ○ ○), MH (▲ ▲ ▲) and TPE (Δ Δ Δ) and in the presence of DETAPAC by MD (● ● ●).

electron donor is indicative of anionic properties of the radical intermediate formed during photosensitisation [22]. Hence as shown in Scheme 1, it is possible that the electron donors, EDTA and DETAPAC may interact effectively with the excited state of quinones leading to the generation of $Q^{-\bullet}$. In the presence of oxygen the latter species, $Q^{-\bullet}$, can yield $O_2^{-\bullet}$.

Photogeneration of superoxide anion was also studied by EPR spin trapping technique. The life time of DMPO-$O_2^{-\bullet}$ adduct is very short in protic solvent such as water and the superoxide adduct readily decomposes to DMPO-OH [23]. Hence, EPR spin trapping studies were carried out in DMSO in which the DMPO-$O_2^{-\bullet}$ adduct has a longer life time [24]. EPR signal was not observed when DMPO alone was irradiated. Also, no EPR signal was identified in the darkness from a sample containing the quinone (100 μM) and DMPO (100 mM) in DMSO solvent (Fig. 6(a)). Fig. 6(b) shows a 12-line EPR spectrum observed upon photoirradiation of a sample consisting of TP (100 μM) and DMPO in air saturated DMSO. This EPR spectrum, characteristic of the $O_2^{-\bullet}$ spin adduct of DMPO, was analysed as a primary nitrogen triplet ($a_N = 1.2$ mT) split by a secondary proton ($a_H^{\beta} = 1.03$ mT) which in turn is further split by a secondary proton ($a_H^{\gamma} = 0.1$ mT). These hyperfine coupling constant values are close to the values reported previously for the same adduct produced on photoirradiation of hypericin (HC)

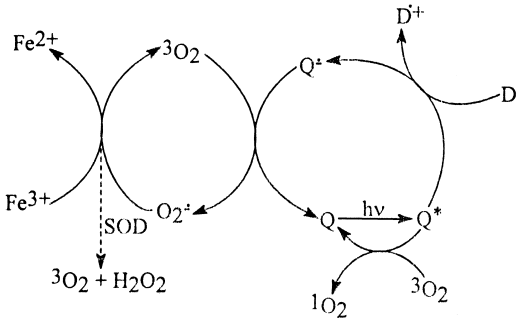

Scheme 1.

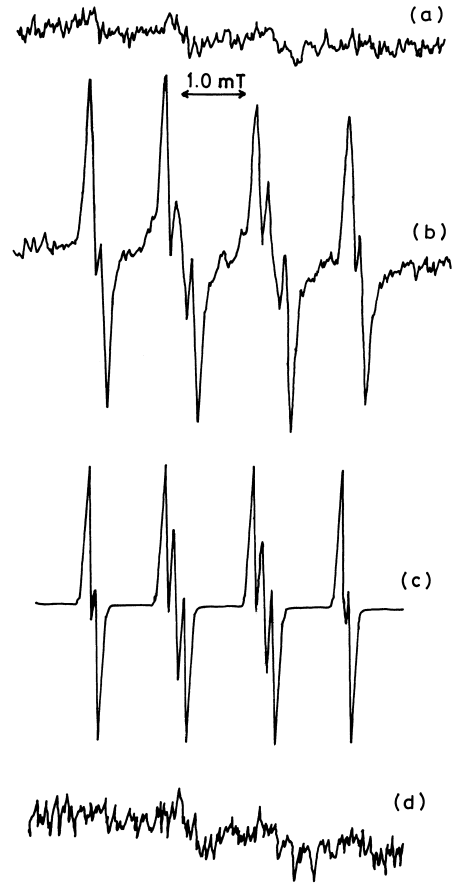

Fig. 6. EPR spectrum of DMPO-$O_2^{-\bullet}$ adduct in air saturated DMSO solution containing TP (100 μM) and DMPO (100 mM) (a) in dark (b) after irradiation (c) the simulated spectrum of DMPO-$O_2^{-\bullet}$ adduct using $a_N = 1.2$ mT; $a_H^{\beta} = 1.03$ mT, $a_H^{\gamma} = 0.1$ mT and (d) in the presence of SOD (50 μg/ml).

in DMSO [22]. Computer simulation using above hyperfine coupling constants gives a spectrum (Fig. 6(c)) which is identical with the experimental spectrum. The control experiments confirmed that quinone, oxygen and light are all necessary to produce the spin adduct. Addition of SOD prior to illumination prevents the formation of spin adduct as shown in Fig. 6(d). Similar DMPO-$O_2^{-\bullet}$ adduct was detected when other quinones MD, TPE and MH were also photolysed in the presence of DMPO in DMSO solution. Thus the spin trapping experiments also confirmed the formation of $O_2^{-\bullet}$ upon photolysis of TP, MD, MH and TPE.

During photolysis of MH in the absence of DMPO both light dependent and intrinsic radicals (dark) were seen as shown in Fig. 7(a) and (c). These two radicals have different *g*-values. The *g*-values are found to be 2.0031 and 2.0028 for intrinsic and light induced radicals, respectively. A computer simulated spectrum (Fig. 7(b)), obtained by the summation of these two radicals, matches well with the experimentally observed one (Fig. 7(a)). Attempts were also made to follow the time dependence of the photogeneration and dark decay of the radicals. MH caused an immediate generation of the signal, which reached a steady state level in approximately

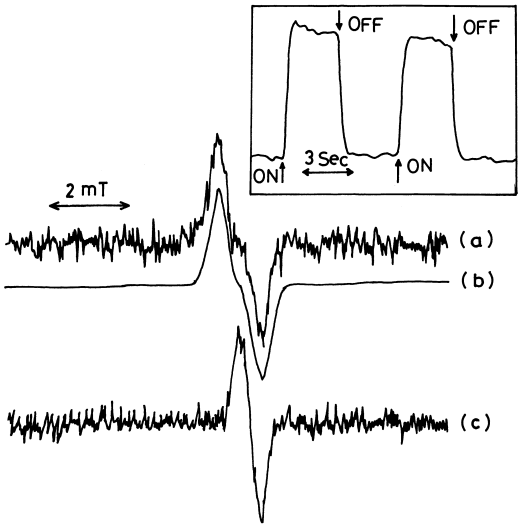

Fig. 7. EPR spectrum of a radical intermediate of MH in DMSO (a) during irradiation (c) in the dark. (b) The simulated spectrum obtained by the summation of both light dependent and intrinsic radicals. Inset in (a) shows kinetics of photogeneration and decay of the radical intermediate. Arrows indicate when light is turned ON (↑) or OFF (↓).

3 s from the beginning of exposure (Inset of Fig. 7(a)). As the light was switched off, the intensity of the EPR signal decreased. The initial portion of the decay curve may be described by second order kinetics. Earlier studies on photolysis of melanins (redox polymer containing *o*-quinone and *o*-hydroquinone groups) revealed the formation of semiquinone radical as a key intermediate [25]. This radical was formed rapidly and the time profile of the EPR spectrum revealed spin polarisation effect characteristic of triplet state involvement. Due to lack of the facility of a time resolved EPR spectrometer, we are unable to carry out a similar investigation. Nevertheless, it seems likely that photolysis of MH also may involve a semiquinone radical.

It is of interest to compare the present results with our earlier study [10] in which these quinones were tested for their cytotoxicity against human breast adenocarcinoma cells (MCF-7). The cytotoxicity followed the order MD > TP > MH ≅ TPE. However, the oxygen consumption rate of these quinones during enzymatic reduction followed the order TP > MD > MH ≅ TPE which is the order of the redox potentials of these quinones. In a similar way, it is interesting to note that the order of photosensitising efficiency of quinones to generate $O_2^{-\cdot}$ and $^1O_2$ (TP > MD > MH ≅ TPE) also follows the same order of oxygen consumption rate.

Although TP is found to be very efficient in the generation of reactive oxygen species, for a potential phototherapeutic agent the absorption at red is an important requirement [26]. Derivatisation of these quinones to achieve red absorption, without affecting the quinone moiety, will be the subject of future reports.

Acknowledgements

Thanks are due to the Department of Science and Technology, New Delhi, India for financial assistance. We are grateful to Dr. M.K. Cherukuri, NIH, for EPR facility and many fruitful discussions.

References

[1] A. Blem, L.I. Grossweiner, Photochem. Photobiol. 41 (1985) 27.
[2] D. Kessel, Photochem. Photobiol. 44 (1986) 489.
[3] K. Reszka, P.G. Tsoungas, J.W. Lown, Photochem. Photobiol. 55 (1992) 359.
[4] K. Reszka, P. Kolodziejczyk, J.W. Lown, Free Radic. Biol. Med. 2 (1986) 267.
[5] J.A. Hartley, K. Resaka, J.W. Lown, Free Radic. Biol. Med. 4 (1988) 337.
[6] Z.J. Diwu, R.P. Haugland, J. Liu, J.W. Lown, G.G. Miller, R.B. Moore, K. Brown, J. Tulip, M.S. Mc phee, Free Radic. Biol. Med. 20 (1996) 589.
[7] K.J. Reszka, D. Bilshi, G.F. Chignell, J.A. Hartley, N. Khan, R.L. Souhami, A.J. Mendonea, J.W. Lown, J. Photochem. Photobiol. 15 (1992) 317.
[8] K.J. Reszka, P. Kolodziejczyk, J.W. Lown, Free Radic. Biol. Med. 5 (1986) 63.
[9] Z.J. Diwu, J.W. Lown, Free Radic. Biol. Med. 18 (1995) 357.
[10] J. Johnson Inbaraj, R. Gandhidasan, R. Murugesan, Free Radic. Biol. Med. (1998), in press.
[11] S. Neelakantan, V. Rajagopalan, P.V. Raman, Indian J. Chem. 22B (1983) 95.
[12] B. Kalyanaraman, C.C. Felix, R.C. Sealy, Photochem. Photobiol. 36 (1982) 5.
[13] I. Kraljic, S. El Mohsni, Photochem. Photobiol. 28 (1978) 577.
[14] E. Gandin, Y. Lion, A. Van De Vorst, Photochem. Photobiol. 37 (1983) 271.
[15] E. Gandin, Y. Lion, J. Photochem. 20 (1982) 77.
[16] P.C.C. Lee, A.J. Rodgers, Photochem. Photobiol. 45 (1987) 79.
[17] W.H. Koppenol, J. Butler, Isr. J. Chem. 24 (1984) 11.
[18] F. Wilkinson, J.G. Brummer, J. Phys. Chem. Ref. Data 10 (1981) 809.
[19] W. Bors, C. Michel, M. Saran, Eur. J. Biochem. 95 (1979) 621.
[20] H.C. Sutton, G.F. Vile, C.C. Winterbourn, Arch. Biochem. Biophys. 256 (1987) 462.
[21] B. Kalyanaraman, E. Perez-Reyes, R.P. Mason, Biochim. Biophys. Acta 630 (1980) 119.
[22] Z. Diwu, Free Radic. Biol. Med. 14 (1993) 209.
[23] E. Finkelstein, G.M. Rosen, E.J. Rauckman, Mol. Pharmac. 21 (1982) 262.
[24] E. Ben-Hur, A. Carmichael, P. Riesz, I. Rosenthal, Int. J. Radiat. Biol. 48 (1985) 837.
[25] C.C. Felix, J.S. Hyde, R.C. Sealy, Biochem. Biophys. Res. Commun. 88 (1979) 456.
[26] C.J. Gomers, Photochem. Photobiol. 54 (1991) 1093.